Measurement of optical flatness using electronic levels

Julius Yellowhair
Sandia National Laboratories
1515 Eubank SE
Albuquerque, New Mexico 87123
E-mail: jeyello@sandia.gov

James H. Burge, FELLOW SPIE
University of Arizona
College of Optical Sciences
1630 East University Boulevard
Tucson, Arizona 85721

Abstract. Conventional measurement methods for large flat mirrors are generally difficult and expensive. In most cases, comparison with a master or a reference flat similar in size is required. Using gravity, as in modern pendulum-type electronic levels, takes advantage of a free reference to precisely measure inclination or surface slopes. We describe using two electronic levels to measure flatness of large mirrors. We provide measurement results on a 1.6-m-diameter flat mirror to an accuracy of 50 nm rms of low-order Zernike aberrations. [DOI: 10.1117/1.2831131]

Subject terms: slope testing; metrology; electronic levels; large flat mirrors; optical manufacturing.

Paper 070194R received Mar. 3, 2007; revised manuscript received Aug. 20, 2007; accepted for publication Aug. 24, 2007; published online Feb. 28, 2008.

1 Introduction

Traditionally, testing large flat mirrors (>1-m diameter) can be difficult and expensive. A test that is normally performed on large flat mirrors is the Ritchey-Common (RC) test.[1] This requires a reference spherical mirror larger in size than the test surface; thus the test accuracy is limited to the accuracy of the spherical mirror. The RC test is straightforward on a small scale; however, aligning large optical components is a difficult and time-consuming process. The effect on schedule makes this test expensive for large optics. To overcome this problem, we introduce a simple and cost-effective slope test that uses two high-precision electronic levels to measure flatness of large mirrors.

Since the mid-1900s, techniques have been developed to measure flatness of surfaces, namely, industrial surface plates.[2] Methods to estimate the uncertainty in the measurements so as to calibrate the surface plates have also been developed.[2,3] The first flatness measurement instruments included an autocollimator and a sliding mirror aligned to it. The autocollimator measured angle deviations on the surface by sliding the mirror over it along measurement lines. Height profiles were obtained by integrating the measured angle deviations or slopes.

In the 1990s high-precision electronic levels were introduced and became commercially available. The measuring principle of electronic levels is based on a friction-free pendulum suspended between two electrodes. A deflection of the pendulum changes the capacitance between the electrodes, which is detected by a transducer and translated to an angle reading. Electronic levels have started to replace the autocollimator and mirror for measuring flatness of surfaces. One benefit of electronic levels, in this case, is that their use does not require the skill needed to operate an autocollimator. The angle readings can be recorded from a digital display or a data acquisition system.

At the University of Arizona, we extended the concept of measuring flatness of surface plates to optical surfaces. A significant advantage of using electronic levels for surface measurements of large mirrors during fabrication is that the mirror can remain on the polishing supports. In contrast, other types of test systems may require moving the test mirror to a testing fixture. In addition to measurement efficiency, their ease of use and low cost make the electronic levels ideal for flatness measurements of large mirrors during the early stages of manufacturing.

In Sec. 2 we introduce the concept of using single-axis electronic levels for large flat mirror measurements. In Sec. 3 we provide the sensitivity and error analysis. Next, in Sec. 4 we provide results of flatness measurements on a 1.6-m-diameter flat mirror and a comparison with another slope test. Finally, in Sec. 5, we describe a conceptual implementation of dual-axis electronic levels for flatness measurements on large flat mirrors. We also present a simulation of dual-axis electronic levels for surface measurements.

2 Test Concept

2.1 *Principles of Operation*

A single electronic level measures the inclination of a surface, α, very accurately. A schematic of a measurement of an inclined surface is shown in Fig. 1. Two levels used

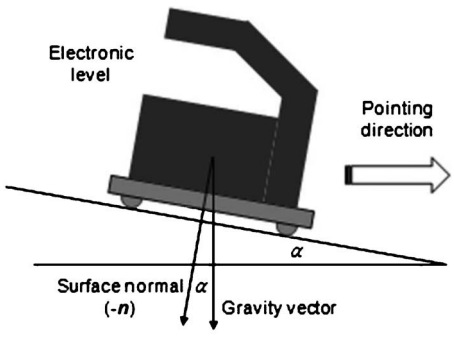

Fig. 1 Setup for measuring inclination with the electronic level.

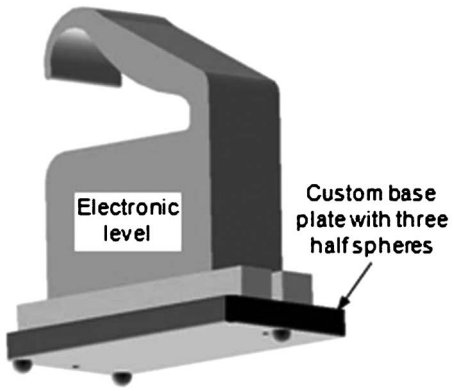

Fig. 2 Electronic level with a custom aluminum three-point base plate.

differentially allow for slope measurements along the pointing direction, where one level provides the reference measurement, B, and the other level provides the measurement A. The differential measurement, A minus B, removes common surface tilt and motion. The reference level is normally fixed while level A is moved over the surface maintaining the common pointing of both levels. The scanning level is placed at several positions along the scan line.

We procured two high-precision single-axis electronic levels (Leveltronic, made by Wyler AG) along with the necessary hardware and electronics. Single-axis, as opposed to dual-axis, levels can only measure inclination in the pointing direction. We replaced the standard steel base plates with custom aluminum plates and three tungsten carbide half spheres as shown in Fig. 2. The half spheres made stable point contacts with the optical surface. Maintaining the pointing of both levels is important when measuring the flatness of a surface as shown in Fig. 3. To ensure line scans, a fiberglass guide rail was fabricated that fitted over the flat mirror. The guide rail ensured consistent pointing of the levels and repeatability of the measurement locations. Typically, we sampled the 1.6-m-diameter mirror with 12 measurement points across it, with a higher measurement density near the edges. The purpose of concentrating on the edges was to monitor them during grinding and coarse polishing of the mirror. A LabVIEW program was developed for data acquisition. The slope data, measurement positions on the mirror, and other measurement parameters (mirror diameter, scan offset from the center of the mirror, etc.) were saved into a text file. The text file was then read in by the analysis software, which reduced the slope data to low-order Zernike aberrations through a least-squares calculation.

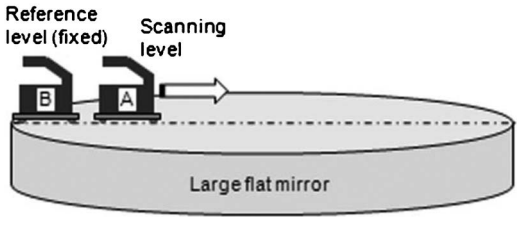

Fig. 3 Schematic of differential slope measurement on an optical surface using two electronic levels.

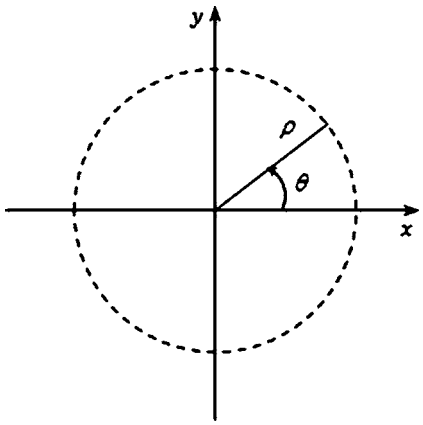

Fig. 4 Coordinate system for defining the Zernike polynomials (ρ is the normalized radial coordinate, and θ is the measurement direction).

2.2 *Zernike Polynomials Fitted to Slope Data*

Since the electronic levels measured slope change, we performed the analysis using a basis set of slope functions derived from the Zernike polynomials. If the surface error is described by

$$S(x,y) = \sum a_i Z_i(x,y) \tag{1}$$

and measurements are made in a direction defined by

$$\hat{\mathbf{i}} \cos\theta + \hat{\mathbf{j}} \sin\theta, \tag{2}$$

then the slope data can be expressed as

$$\alpha(x,y,\theta) = \sum a_i \nabla Z_i(x,y) \times (\hat{\mathbf{i}} \cos\theta + \hat{\mathbf{j}} \sin\theta), \tag{3}$$

where ∇ is the gradient operator, Z_i are the Zernike polynomials, and a_i are the coefficients. The analysis software created a matrix of low-order slopes and a vector of measured surface slopes. Through a least-squares calculation, the Zernike coefficients were determined by

$$[\mathbf{a}] = [\boldsymbol{\alpha}] \backslash [\mathbf{z}'], \tag{4}$$

where $[\mathbf{z}']$ is a matrix of low-order slopes derived from the Zernike polynomials projected in the measurement direction, and $[\boldsymbol{\alpha}]$ is a vector of measured slope variations across the mirror surface. The \ operator was used in MATLAB[4] for the least-squares fit. After the coefficients were determined, the Zernike polynomials were used to reconstruct the surface topology map of the flat mirror.

3 Analysis

3.1 *Sensitivity Analysis: Sampling for Low-Order Zernike Aberrations*

A single line scan across the mirror does not sample all the low-order Zernike aberrations shown in Table 1. Figure 4 shows the geometry for defining the Zernike aberrations.

Table 1 List of the low-order Zernike polynomials (UofA).

Aberration	Zernike polynomial	Gradient
Power	$Z4=2(x^2+y^2)-1$	$4x\hat{\mathbf{i}}+4y\hat{\mathbf{j}}$
Astigmatism	$Z5=(x^2-y^2)$	$2x\hat{\mathbf{i}}-2y\hat{\mathbf{j}}$
	$Z6=2xy$	$2y\hat{\mathbf{i}}+2x\hat{\mathbf{j}}$
Coma	$Z7=3(x^3+xy^2)-2x$	$(9x^2+3y^2-2)\hat{\mathbf{i}}+6xy\hat{\mathbf{j}}$
	$Z8=3(x^2y+y^3)-2y$	$6xy\hat{\mathbf{i}}+(3x^2+9y^2-2)\hat{\mathbf{j}}$
Spherical	$Z9=6(x^4+y^4)-6(x^2+y^2)+1$	$12x(2x^2-1)\hat{\mathbf{i}}+12y(2y^2-1)\hat{\mathbf{j}}$
Trefoil	$Z10=x^3-3xy^2$	$3(x^2+y^2)\hat{\mathbf{i}}-6xy\hat{\mathbf{j}}$
	$Z11=3xy^2-y^3$	$6xy\hat{\mathbf{i}}+3(x^2-y^2)\hat{\mathbf{j}}$

The non-rotationally-symmetric aberrations have orthogonal components, cosine and sine. Measuring for both components of astigmatism, for example, requires three line scans in different directions [e.g., three line scans separated by 120 deg as shown in Fig. 5(c)]. Three scans also allow averaging for power. Figure 5 shows other types of sampling arrangements to measure the low-order aberrations. Scans through the center of the mirror are not required. The scans can be offset from center; the aberrations measured still hold for the number of line scans made. The mirror surface should be well sampled along each scan line to avoid aliasing of the surface modes.

Figure 6 demonstrates how the slope measurements would appear for the low-order aberrations if three line scans (at 0, 120, and 240 deg) shown in Fig. 5(c) were performed. The plots are normalized by assuming the Zernike wavefront coefficients are 1 μm. The amount of each low-order term is determined using the least-squares fit to the measured slope data. The three line scans have excellent sensitivities to the low-order aberrations, except for Zernike 11. Trefoil is thus not adequately sampled with the three line scans. However, the four line scans shown in Fig. 5(d) remedy this.

3.2 *Error Analysis*

Drescher[2] reported on a method for estimating uncertainty in the surface slope measurements of industrial surface plates. We applied a similar analysis. The error sources can be separated into two categories: random and systematic errors. The random errors can be controlled through data averaging. The systematic errors are fixed.

3.2.1 *Random errors*

1. In addition to inherent noise associated with the electronic levels, there was also a drift effect due to the environment, notably thermal. The magnitude and direction of the drift depended on the temperature gradient at the base plates of the levels. Figure 7 represents a continuous measurement that shows drift and noise for a positive temperature gradient at the base plate of one level. The levels were placed on the mirror surface after rinsing the mirror of the polishing compound with filtered tap water and allowed to settle and equilibrate for one hour. Measurements were then continuously taken over another hour from one level at the full sampling rate of the device (3.3 Hz). The other level exhibited similar behavior. A temperature gradient (mirror top surface to ambient room temperature, controlled to ± 0.6 K) still existed even after 2 h.

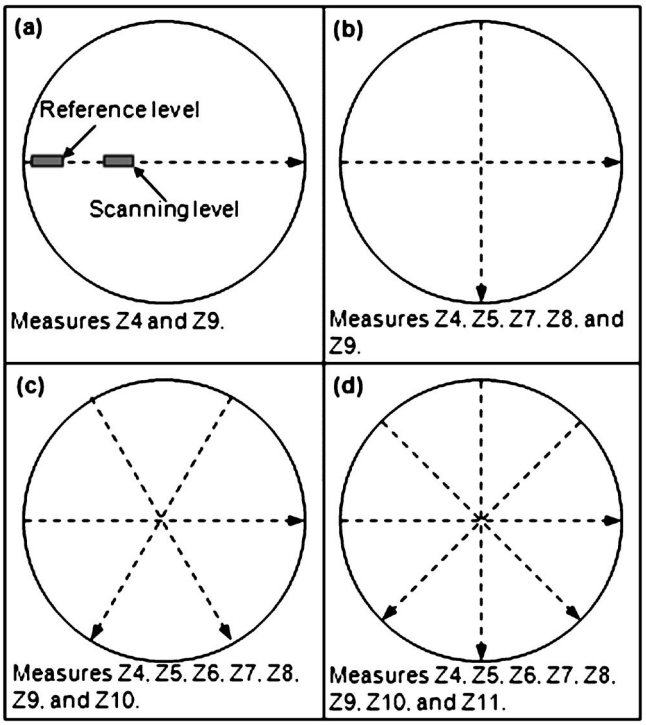

Fig. 5 Sampling requirements for measuring low-order Zernike aberrations.

The plot shows the levels drifted about 1.75 μrad over 1 h. To minimize the drift effect, a reference measurement was made that accompanied the data point. The reference measurement consisted of placing the scanning level next to the fixed level and taking a measurement. The scanning level was then moved back to the actual measurement location, and a measurement was taken. The reference measurement was then subtracted from the datum. This procedure was repeated for all the acquired data points. The reference and actual measurements were acquired in rapid succession at intervals much less than the time constant of the drift. For example, acquiring both measurements in 3 min introduced about 90 nrad of slope error.

2. There was inherent noise in the electronic levels. We measured the noise floor of the levels to less than 0.2 μrad (at 1 standard deviation). Figure 8 shows the continuous measurement from Fig. 7, exhibiting noise after removing the linear drift effect.

3. The fiberglass guide rail was not perfectly straight. The straightness was specified to 0.5 mm/m. This caused an error in pointing and coupling of the reading between the orthogonal axes; thus the slope error in x became

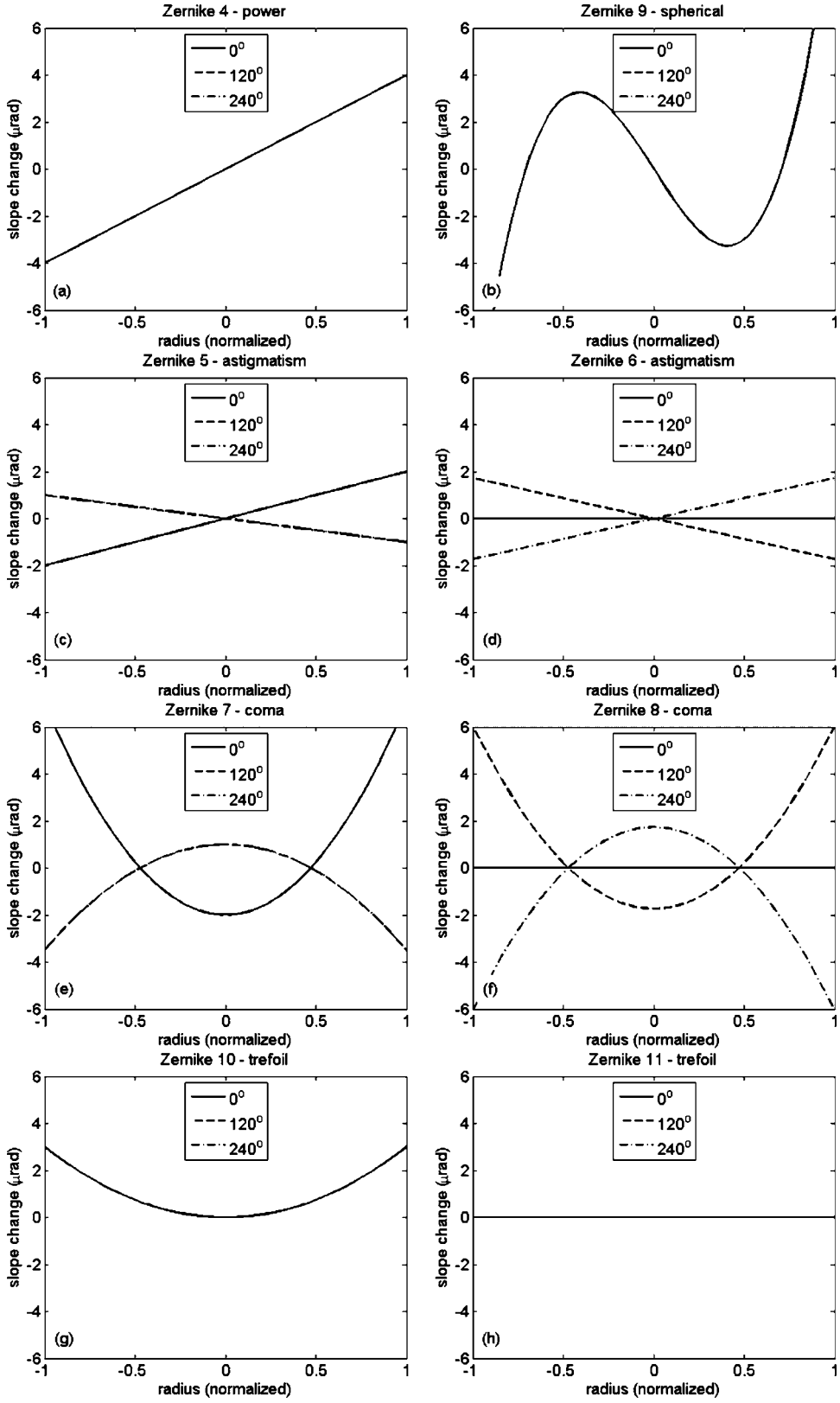

Fig. 6 Three simulated line scans (separated by 120 deg) for low-order surface errors described by single Zernike polynomial terms.

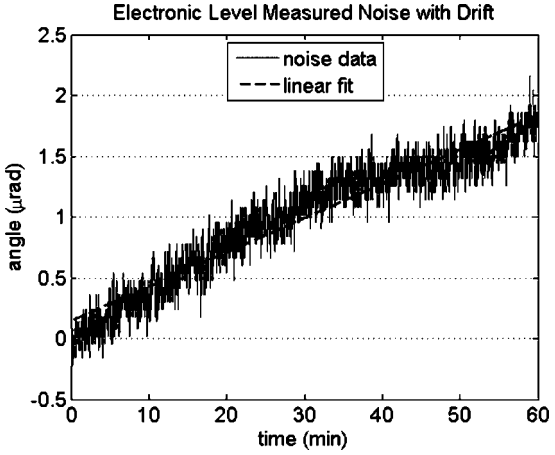

Fig. 7 Measured drift and noise over 60 min. The amount of drift is about 1.75 μrad (30 nrad/min).

$$\Delta\alpha_x = \alpha_y \Delta\theta, \tag{5}$$

where α_y is the slope in y and $\Delta\theta$ is the error in pointing. During coarse polishing, we assumed the mirror surface slopes varied by 4 nrad/mm. The contact-point spacing of the electronic levels in the y direction was 64 mm; thus the slope in y varied by 256 nrad. The error in the slope reading in x was then 0.13 μrad.

4. The slope error due to placement or setting of the levels is described by

$$\Delta\alpha = \left[\left(\frac{d\alpha_x}{dx}dx\right)^2 + \left(\frac{d\alpha_y}{dy}dy\right)^2\right]^{1/2}. \tag{6}$$

The guide rail helped in constraining the placement of the levels to 2 mm in the pointing (x) direction and to 0.5 mm in the y direction. If the surface slopes varied by 4 nrad/mm, then the placement error caused about 8 nrad.

3.2.2 *Systematic errors*

There are two systematic errors to consider:

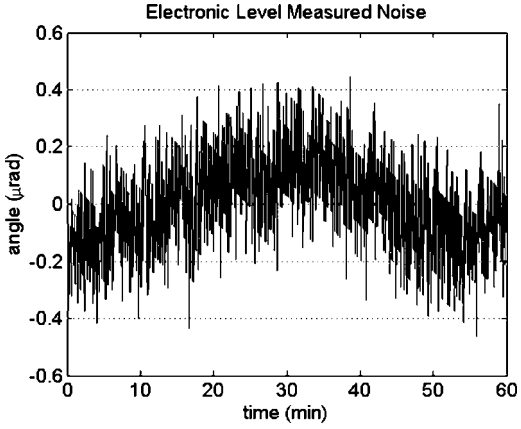

Fig. 8 Measured noise in the electronic levels after removing linear drift (σ=0.15 μrad). Sample period 3.3 Hz (full rate).

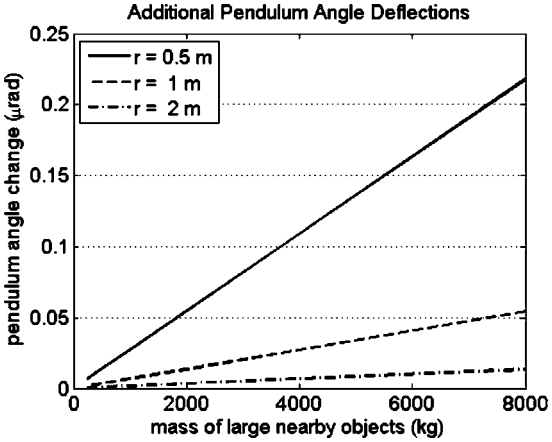

Fig. 9 Simulated changes in pendulum angle due to force of attraction between the pendulum and nearby large objects.

1. The residual error from the slope fit calculation introduced an uncertainty as much as 0.13 μrad.
2. Gravity effects on the pendulum may introduce an additional angle deflection. We assumed the level pendulum always pointed in the direction of gravity for reference. However, the force of attraction between the pendulum and a nearby large object can cause an additional deflection to the pendulum, thus changing the slope measurements.

The attracting force between two objects is given by

$$F = G\frac{m_1 m_2}{r^2}, \tag{7}$$

where G is the gravitational constant, m_1 and m_2 are the masses of the two objects, and r is the distance between them. The force in Eq. (7) on the pendulum can cause an additional deflection by amounts shown in the plot in Fig. 9.

The plot shows, however, that an object must be about 7000 kg (8 tons) and only 0.5 m away to have a noticeable effect on the slope measurements. The only large object in

Table 2 Sources of error for slope measurements (for a single level).

Error source	Value (μrad)
Noise in the levels and calibration	0.25
Drift due to environment	0.10
Axis coupling (guide rail)	0.13
Level placement and setting	0.01
Software fit error (residual)	0.13
Gravity	0.10
Total error (root sum square)	0.34

Table 3 Measurement accuracy for the low-order Zernike aberrations with the uniaxial levels.

Zernike aberration	Measurement accuracy, rms (nm)
Power	16
cos astigmatism	29
sin astigmatism	29
cos coma	11
sin coma	11
Spherical	8
Secondary spherical	6
Root sum square	50

close proximity to the mirror was the polishing machine, which weighed about 2,700 kg (3 tons). The force of attraction between the polishing machine and the level pendulum would then cause an error of less than 0.1 μrad.

3.2.3 *Monte Carlo analysis*

Table 2 shows a summary of the sources of errors and their values. After combining all the error sources, the total error is about 0.34 μrad from a single level. A Monte Carlo simulation of the three line scans [Fig. 5(c)] on a 2-m flat mirror was performed to determine the uncertainty in measuring the low-order Zernike aberrations, using an error of 0.48 μrad for a differential measurement and 12 measurement points per scan. Table 3 shows the result of the simulation. The expected accuracy for measuring a 2-m mirror is about 50 nm (rms) of low-order aberrations. Separately, power can be measured to an accuracy of about 16 nm (rms) with this measurement method.

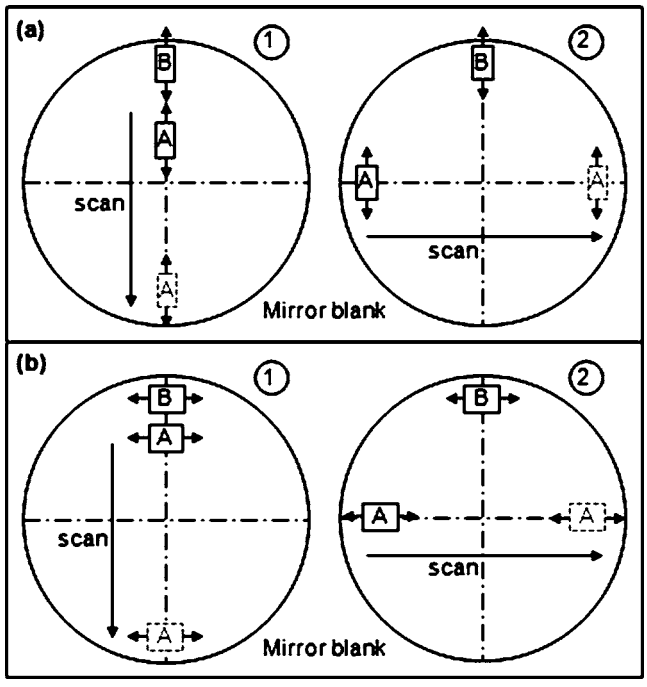

Fig. 10 Orthogonal scans with (a) up-down and (b) left-right pointing directions using single-axis electronic levels.

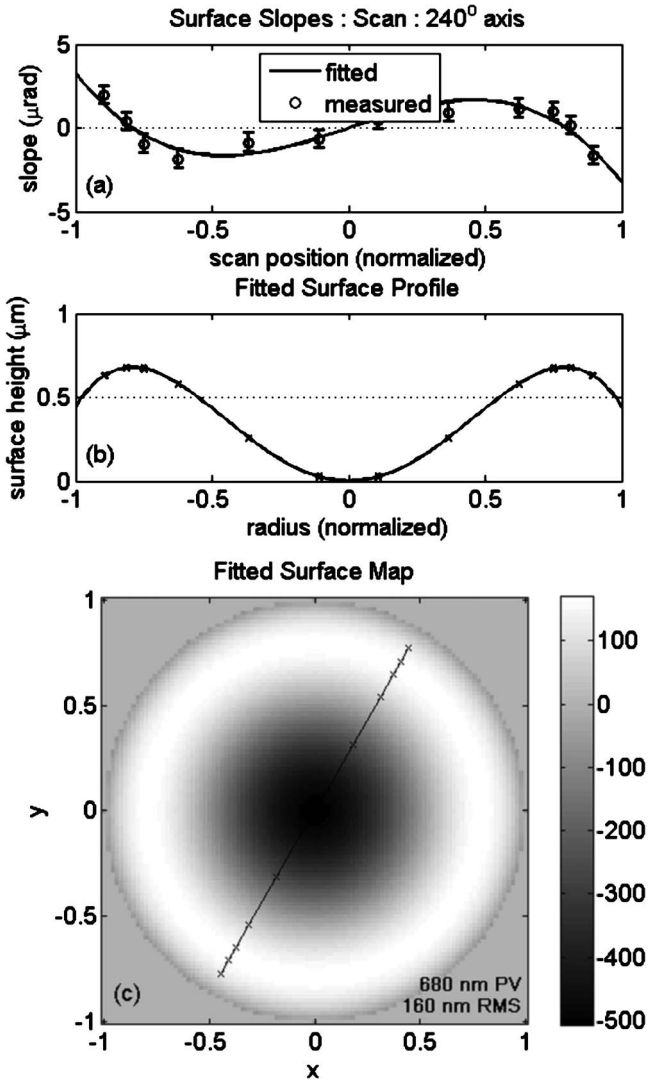

Fig. 11 (a) Low-order rotationally symmetric Zernike aberrations fitted to measured slope data. (b) Surface profile of the fitted surface map. (c) The corresponding two-dimensional fitted surface map with 680 nm peak to valley and 160 nm rms.

3.3 *Other Scanning Arrangements for Single-Axis Electronic Levels*

Other scanning arrangements are possible for measuring surface slopes in large flat mirrors using single-axis electronic levels. Figure 10 shows orthogonal scans with (a) up-down and (b) left-right pointing directions. The analysis remains the same for these scanning arrangements.

4 Measurement of a 1.6-m Flat Mirror

4.1 *Single Line Scan*

A single line scan, as shown in Fig. 5(a), samples only rotationally symmetric aberrations (e.g., power). Figure 11

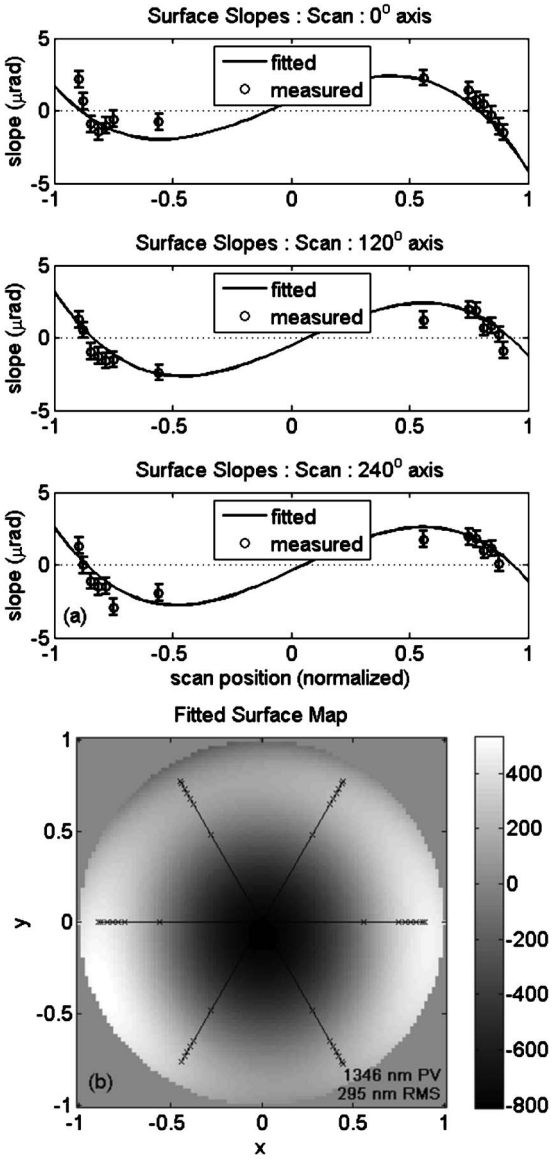

Fig. 12 (a) Fit to measured surface slopes along three lines separated by 120 deg. (b) The resulting surface map of the three line scans (295 nm rms).

shows the result of a single line scan on the 1.6-m mirror during fabrication. The top plot (a) shows the measured surface slopes and a fit to them using the slope functions derived from the Zernike polynomials for power and spherical aberration. The middle plot (b) shows the surface profile after determining the Zernike coefficients through the least-squares fit to the slope data. The bottom plot (c) shows the reconstructed surface map and the scan made on the mirror. All of the plots are normalized in radius. The results shown in Fig. 11 yielded an overall surface error (rms) of 160 nm: 127 nm power and 128 nm spherical aberration.

4.2 *Three Line Scans*

Three line scans, as shown in Fig. 5(c), provided information on all the low-order Zernike aberrations, except for trefoil. Figure 12(a) shows the result of the three line scans on the same 1.6-m flat mirror (at a different time in the manufacturing process) and fits to them using the low-order slope functions. Figure 12(b) shows the reconstructed surface map after fits to the measured surface slopes and the line scans made on the mirror. The map yielded 295 nm of overall rms surface error. Table 4 shows a breakdown of error contributions from the low-order aberrations.

Table 4 Values of the low-order Zernike coefficients after fit to surface slopes.

Zernike aberration	Value, rms (nm)
Power	280
cos astigmatism	–97
sin astigmatism	33
cos coma	–65
sin coma	6
Spherical	–141

4.3 *Comparison with the Scanning Pentaprism Test System*

In this subsection, we provide a comparison of the test with electronic levels and the test with scanning pentaprisms, which used two pentaprisms coaligned with a high-resolution electronic autocollimator. Both test systems measured surface slopes, with the scanning-pentaprism test providing higher measurement accuracy.[5,6] To validate the measurements with the electronic levels, the 1.6-m flat was measured with both test systems while the mirror was in early production. The same direction on the mirror was measured, and 10 measurement points across the mirror were acquired with both test systems. The measurement spacing between the two systems differed, however.

Figure 13 shows the results from the electronic-level test, and Fig. 14 shows the results from the scanning-pentaprism test. Table 5 shows (for comparison) the rms surface statistics from both tests after the slope functions for power and spherical aberration were fitted to the slope data. In addition to the different sampling spacing, the measurements with the electronic levels and with the scanning pentaprism differed for two other reasons:

1. The rms measurement accuracy of the electronic levels was limited to about 16 nm for power and 8 nm for spherical aberration (as shown in Sec. 3.2.3). That of the scanning pentaprism was 9 nm for power and 2 nm for spherical aberration.[6]
2. The measurement sampling length is about 40 mm for the scanning pentaprism (spot size on the test mirror), and about 140 mm for the electronic levels (contact-point spacing in the measurement direction). This causes the same effect as averaging the surface slopes over the measurement sampling length, but it is less of a problem for measuring low-order aberrations.

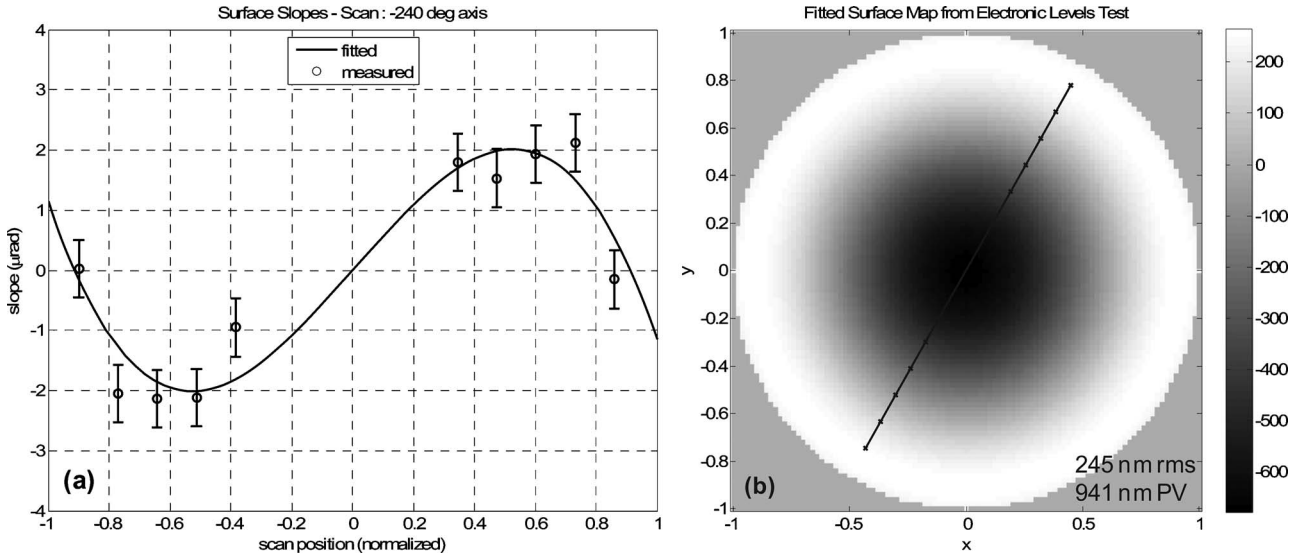

Fig. 13 Measurements on the 1.6-m flat with electronic levels. (a) Slope measurements and fit to the slope data. (b) A fitted surface map after determining the Zernike coefficients through a least-squares fit.

The results of the comparison show that the two test systems agree to within the measurement accuracy of the electronic levels for power, thus validating the electronic-level measurements. The measurement for spherical aberration with the electronic levels is much smaller, due to the averaging effect just described, and because the edge point that was measured with the scanning pentaprism test gave it more weight for the spherical aberration fit.

5 Implementation with Dual-Axis Electronic Levels

The alternative scanning arrangements given in Sec. 3.3 can be accomplished more efficiently with dual-axis electronic levels as shown in Fig. 15. Dual-axis levels can measure inclination about two orthogonal axes simultaneously. Although we did not procure dual-axis levels during the work reported here, they are available commercially. In this section, we analyze the performance of such levels through Monte Carlo simulations, assuming the same type of measurement accuracies for both axes as for the single-axis levels.

The data reduction remains the same. Slopes in orthogonal directions will now be known for each measurement point; the common pointing of the levels must still be maintained. The errors contributing to uncertainty in the measurement can be treated in the same manner as for the single-axis levels. With dual-axis levels, measurements on

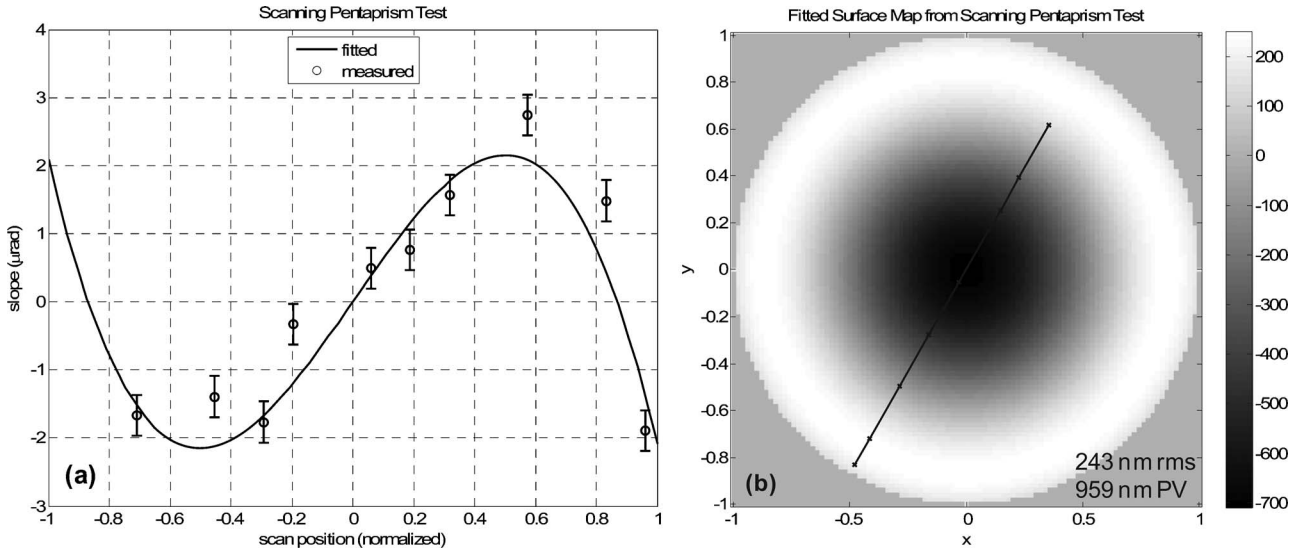

Fig. 14 Measurements on the 1.6-m flat with the scanning pentaprism. (a) Slope measurements and fit to the slope data. (b) A fitted surface map after determining the Zernike coefficients through a least-squares fit.

Table 5 Zernike coefficients for power (Z4) and spherical aberration (Z9) after fits to the slope data from the electronic levels and scanning pentaprism tests.

Abberation	Electronic levels, rms (nm)	Scanning pentaprism, rms (nm)	Difference, rms (nm)
Power	261	248	13
Spherical	−101	−125	24
Surface	245	243	2

a square grid can be made instead of scans through the center of the mirror, to take advantage of the slope information with respect to orthogonal axes.

Figure 16 shows the results of two measurement simulations with dual-axis electronic levels. Accomplishing the same scans with the single-axis levels would require making additional line scans, demonstrating that dual-axis levels can increase measurement efficiency. Due to this fact, we are interested in obtaining dual-axis electronic levels to do flatness measurements on large flat mirrors in the future.

6 Conclusion

The conventional measurement methods for large flat mirrors are often difficult and expensive. We have provided an analysis of a high-precision electronic-level measurement system that uses gravity as a free reference and measures flatness of large flat mirrors with an option to measure other low-order aberrations. The sources of error that limit the accuracy of the system were quantified; the errors were minimized through data averaging and making reference measurements. A Monte Carlo simulation was performed, based on the measurement uncertainty estimated from the error analysis. The simulation result showed the uncertainty in the measured low-order Zernike aberrations, and measurements to 50 nm rms of low-order aberrations are achievable for 2-m flat mirrors. The accuracy, efficiency, and low cost of the test system are ideal for testing of large flat mirrors. This test system can be used to guide polishing during the early stages of manufacture. In addition, the portability of the test system allowed testing of the flat while on polishing supports instead of in a testing fixture.

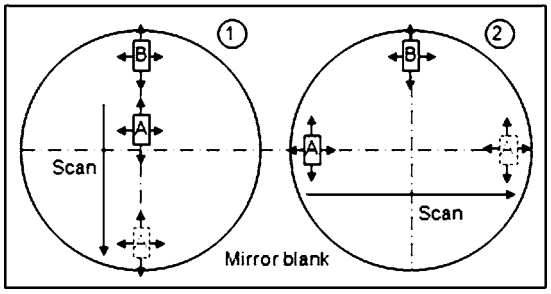

Fig. 15 Simultaneous orthogonal measurements with dual-axis levels.

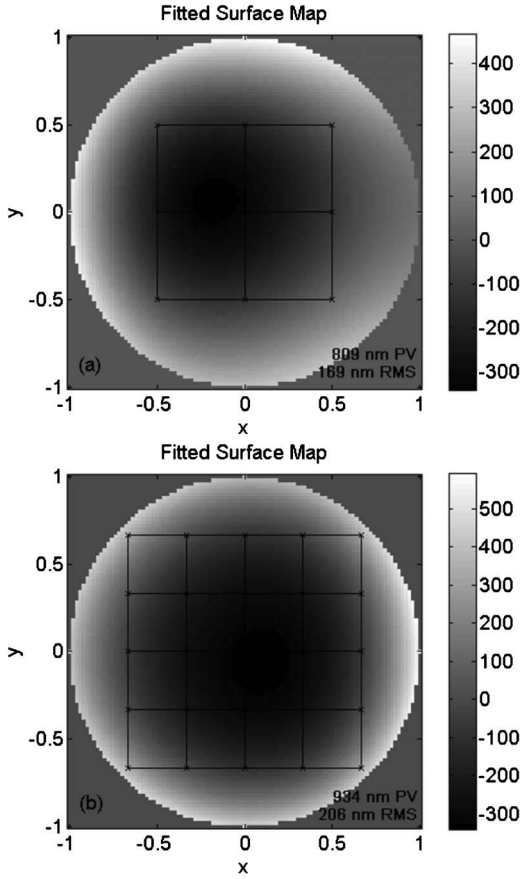

Fig. 16 A simulation result of dual-axis level measurement on (a) 3×3 and (b) 5×5 square grids, assuming the same measurement uncertainty as for the single-axis levels.

References

1. J. Ojeda-Castaneda, "Foucault, wire, and phase modulation tests," in *Optical Shop Testing*, 2nd ed., D. Malacara, Ed., pp. 265–320, Wiley, New York (1992).
2. J. Drescher, "Analytical estimation of measurement uncertainty in surface plate calibration by the Moody method using differential levels," *Precis. Eng.* **27**, 323–332 (2003).
3. B. Acko, "Calibration of electronic levels using a special sine bar," *Precis. Eng.* **29**(1), 48–55 (2004).
4. Mathworks, "MATLAB and Simulink for technical computing," http://www.mathworks.com.
5. P. Mallik, C. Zhao, and J. H. Burge, "Measurement of a 2-m flat using a pentaprism scanning system," *Opt. Eng.* **46**, 023602 (2007).
6. J. Yellowhair and J. H. Burge, "Analysis of a scanning pentaprism system for measurements of large flat mirrors," *Appl. Opt.* **46**, 8466–8474 (2007).

Biographies and photographs of the authors not available.